International Journal of General Medicine

Dovepress
Taylor & Francis Group

Open Access Full Text Article

ORIGINAL RESEARCH

Composite Markers Predict Functional Outcomes in Basal Ganglia Hemorrhage in Patients with Cerebral Small Vessel Disease

Zhiwen Zha[1], Lei Zhu[1], Chuanqin Yu[1], Tong Gu[1], Chen He[1], Xuke Zhang[2], Meihai Wen[2]

[1]Department of Neurology, The First Hospital of Anhui University of Science & Technology, Huainan, Anhui Province, People's Republic of China; [2]Department of Neurology, Bengbu Medical University, Bengbu, Anhui Province, People's Republic of China

Correspondence: Lei Zhu, Email salimai@126.com

Background: Although the presence of cerebral small vessel disease (CSVD) on neuroimaging closely parallels overall stroke risk, it is still uncertain whether combining these structural markers with blood-based profiles can reliably predict functional outcomes in patients suffering from acute basal ganglia hemorrhage (BGH).

Methods: We enrolled 242 BGH patients admitted between January and December 2024. The least absolute shrinkage and selection operator (LASSO) with ten-fold cross-validation selected candidate predictors. Backward elimination in multiple logistic regression identified independent risk variables and built the final model. Discrimination was assessed by the area under the receiver operating characteristic curve (AUC), calibration by the Hosmer-Lemeshow test and calibration plots. The DeLong test and decision curve analysis evaluated model comparison and clinical utility. A risk stratification chart enabled individualized risk assessment.

Results: Multivariable analysis identified four independent predictors of poor prognosis: total load (adjusted OR = 9.25, 95% CI: 3.52–24.28, P < 0.001), triglyceride-to-high-density lipoprotein cholesterol (TG/HDL-C) ratio (adjusted OR = 8.39, 95% CI: 3.21–21.92, P < 0.001), non-high-density lipoprotein cholesterol ratio (NHHR) (adjusted OR = 4.95, 95% CI: 2.50–9.82, P < 0.001), and systemic inflammation response index (SIRI) (adjusted OR = 3.35, 95% CI: 1.89–5.93, P < 0.001). The prediction model showed excellent discrimination, with an AUC of 0.929 (95% CI: 0.89–0.97). At a cutoff value of 0.29, sensitivity was 86% and specificity was 91%. Evaluation of the model's calibration demonstrated a good concordance between the estimated probabilities and the actual clinical endpoints.

Conclusion: Evaluating BGH patients through an integrated lens of blood-based biomarkers and neuroimaging substantially enhances prognostic clarity. Rather than being considered in isolation, systemic indices such as the TG/HDL-C ratio, NHHR, and SIRI combine with cumulative CSVD severity to independently flag high-risk clinical trajectories.

Keywords: cerebral small vessel disease, basal ganglia hemorrhage, blood biomarkers, prognostic prediction model, total load

Background

Constituting nearly 25% of all cerebrovascular events, spontaneous intracerebral hemorrhage (sICH) frequently leads to fatal outcomes or severe neurological deficits. As a result, those who survive the acute phase face drastic, long-lasting declines in their quality of life.[1] Following the initial acute event, a mere 12 to 39% of survivors successfully recover their ability to live independently.[2] In sICH, the basal ganglia are the most frequent location of hematoma occurrence.[3] Cerebral small vessel disease (CSVD) is commonly regarded as the dominant pathological substrate for sICH, with reports attributing up to 85% of cases to this mechanism.[4] In clinical practice, the main subtypes of CSVD include hypertensive arteriopathy related to chronic hypertension and aging, and cerebral amyloid angiopathy caused by β-amyloid deposition in small cerebral vessels.[5] The diagnosis and monitoring of CSVD rely mainly on neuroimaging. The recognized neuroimaging phenotype consists of multiple distinct morphological changes. These prominent signs involve brain volume reduction, cerebral microbleeds, and lacunes, coupled with dilated perivascular spaces, recent subcortical small infarctions, and white matter hyperintensities driven by presumed vascular mechanisms.[6] Collectively, these

https://doi.org/10.2147/IJGM.S605613
Received: 5 March 2026
Accepted: 29 April 2026
Published: 5 May 2026

neuroimaging hallmarks reflect the cumulative severity of CSVD pathology. Furthermore, existing literature consistently links this aggregate damage to an elevated probability of subsequent cerebrovascular events.[7] Even though earlier investigations examined links between single CSVD imaging features and prognosis after sICH, the biological pathways involved are still not fully clarified. Interactions among endothelial dysfunction, chronic inflammation, and small-vessel pathology may contribute to disease progression and prognosis. As a result, reliable and specific biomarkers for predicting CSVD progression and its impact on sICH outcomes are still lacking.

Currently, prognostic assessment of intracerebral hemorrhage mainly relies on clinical scoring systems, such as the modified intracerebral hemorrhage score (mICH Score), clinical grading scales, and the National Institutes of Health Stroke Scale (NIHSS).[8] However, data on the association between acute-phase biomarkers and three-month outcomes in patients with CSVD who develop basal ganglia hemorrhage (BGH) are limited. Predicting outcomes after a BGH event can often present clinical challenges, partly because understanding remains limited regarding how a patient's baseline CSVD burden interacts with their acute laboratory profile during the early phases of recovery. Exploring this relationship could be highly beneficial. It might not only offer clearer insights into the pathological mechanisms potentially underlying CSVD-related bleeding, but also help establish a firmer foundation for clinical forecasting and targeted therapeutic intervention.

Ultimately, we propose that integrating these two distinct diagnostic domains—the structural (cumulative CSVD burden) and the systemic (acute-phase lipid and inflammatory biomarkers)—may identify high-risk individuals more sensitively than relying on either metric alone. Unlike conventional prognostic scores (eg, mICH score) that primarily depend on clinical and radiological variables, our model incorporates both chronic microvascular damage and acute systemic metabolic-inflammatory status, thereby facilitating early risk stratification. By identifying high-risk individuals, clinicians might accordingly intensify monitoring or implement targeted interventions, potentially reducing the risk of poor prognosis.

Materials and Methods

Patients

From January through December 2024, we consecutively enrolled 242 individuals diagnosed with BGH. All participants were selected from consecutive admissions to the Neurology Department. Inclusion criteria were: (1) age 18–85 years; (2) satisfaction of standard diagnostic criteria for CSVD; (3) confirmation of a basal ganglia hematoma by computed tomography within 24 hours of symptom onset; (4) undergoing brain MRA and routine structural MRI within the first 48 hours after presentation. Exclusion criteria were: (1) primary intraventricular, subarachnoid, or subdural hemorrhage; (2) incomplete MRI data or missing key sequences (eg, susceptibility-weighted imaging); (3) incomplete clinical information or missing modified Rankin Scale scores (mRS); (4) secondary hemorrhage due to identifiable causes (eg, trauma, tumor, or vascular malformation); (5) severe cardiac, hepatic, or renal dysfunction, or malignancy; (6) history of surgical treatment or an indication for surgery before admission.

Clinical Data Collection and Imaging Assessment

The total load of CSVD was evaluated according to established composite neuroimaging scoring guidelines.[9] One point was assigned for each of the following features: (1) at least one lacunar lesion; (2) deep white matter hyperintensity graded ≥2 on the Fazekas scale or periventricular hyperintensity rated 3; (3) one or more microbleeds in deep or subcortical regions; (4) perivascular spaces in the basal ganglia classified as grade 2–4. Thus, the total CSVD score ranged from 0 to 4. Based on previous evidence linking higher scores to increased stroke recurrence risk,[10] we classified patients with scores of 3 or 4 as having severe CSVD burden, and those with scores of 0–2 as having mild-to-moderate burden. Three senior neurologists, blinded to clinical data, independently assessed each feature. Discrepancies were resolved by joint discussion. Interobserver agreement was assessed using Fleiss' Kappa ($\kappa = 0.96$). Baseline demographic and clinical characteristics, laboratory results, and NIHSS scores were obtained from electronic medical records. Ninety days following the acute event, we evaluated the participants' neurological recovery utilizing mRS. A good outcome was defined as mRS 0–2, and a poor outcome as mRS 3–6.

Statistical Analysis

All analyses and graphics were produced using R (version 4.5.1), SPSS (v26.0), and GraphPad Prism (10.1.2). Baseline continuous variables were summarized as means or medians, depending on their distribution. Group comparisons were performed using the independent Student's *t*-test or Mann–Whitney *U*-test, as appropriate. Categorical variables were presented as counts (percentages) and compared using the chi-square test or Fisher's exact test. For predictive modeling, we first applied Least Absolute Shrinkage and Selection Operator (LASSO) regression with ten-fold cross-validation to select candidate variables. The optimal penalty parameter (λ) was determined by cross-validation. Variables retained after LASSO were then entered into a multivariable logistic regression model. We used backward stepwise elimination to obtain the most parsimonious set of predictors. To further verify the stability of the regression coefficients, variance inflation factors (VIFs) were used to diagnose multicollinearity among all independent variables, with a VIF > 5 indicating substantial collinearity. Discrimination was assessed using ROC curves. The area under the curve (AUC) and its 95% confidence interval were estimated with 1000 bootstrap resamples. Calibration was evaluated using the Nagelkerke R^2, Hosmer-Lemeshow test, and calibration plots. For clinical use, we constructed a nomogram based on the final regression coefficients. Decision curve analysis (DCA) quantified the clinical utility, and the DeLong test compared performance between models.

Results

Comparative analyses between the two groups revealed that individuals with poor clinical outcomes exhibited markedly greater burdens of white matter hyperintensity lesions, lacunes, dilated perivascular spaces, cerebral microhemorrhages, and an overall more severe manifestation of CSVD (all P values < 0.05). Furthermore, this group demonstrated significantly increased levels of the triglyceride-to–HDL cholesterol (TG/HDL-C) ratio, non–HDL cholesterol concentration, the ratio of non–HDL cholesterol to HDL cholesterol (NHHR), the systemic inflammatory response index (SIRI), and the derived neutrophil-to-lymphocyte ratio (all P values < 0.05) (Table 1).

To narrow down the twenty-two prospective risk factors, we executed a LASSO penalization model. Through a ten-fold cross-validation strategy, the ideal lambda (λ) tuning metric was set at 0.041, strictly adhering to the one-standard-error guideline. At this value, four predictors with nonzero coefficients were retained: Total load, TG/HDL-C ratio, NHHR, and SIRI (Figure 1). These variables were entered into multivariable logistic regression analysis, which identified all four as independent risk factors for poor prognosis: Total load (adjusted OR = 9.25, 95% CI: 3.52–24.28, P < 0.001), TG/HDL-C ratio (adjusted OR = 8.39, 95% CI: 3.21–21.92, P < 0.001), NHHR (adjusted OR = 4.95, 95% CI: 2.50–9.82, P < 0.001), and SIRI (adjusted OR = 3.35, 95% CI: 1.89–5.93, P < 0.001) (Table 2). The VIF values for total load, TG/HDL-C ratio, NHHR, and SIRI ranged from 1.032 to 1.074, all well below the threshold of 5 (TG/HDL-C: 1.032; NHHR: 1.074; SIRI:1.057; Total load:1.051), indicating no substantial multicollinearity and stable regression coefficient estimates. ROC curve analysis showed that the AUC was 0.720 (95% CI: 0.65–0.79) for total load, 0.743 (95% CI: 0.67–0.81) for TG/HDL-C ratio (cutoff 1.53), 0.779 (95% CI: 0.70–0.86) for NHHR (cutoff 2.19), and 0.770 (95% CI: 0.71–0.83) for SIRI (cutoff 2.02). The combined predictive model achieved an AUC of 0.929 (95% CI: 0.89–0.97). At a cutoff value of 0.29, sensitivity was 86% and specificity was 91% (Table 3 and Figure 2a). To assess overfitting, optimism correction was performed using 1000 bootstrap resamples. The average optimism was 0.0159, and the optimism-corrected AUC was 0.914, indicating negligible overfitting and stable coefficient estimates. The calibration plot, based on 1000 bootstrap resamples, showed that the predicted probabilities were in reasonable agreement with actual outcomes, which was supported by the Hosmer-Lemeshow test (χ^2 = 8.674, P = 0.371) (Figure 2b). The Nagelkerke R^2 was 0.626, indicating a good model fit. The collective predictive value of the four chosen variables was further substantiated by the likelihood ratio test (χ^2 = 134.12, P < 0.001). To bridge the gap between statistics and clinical practice, we rendered this multivariable framework into a visual nomogram for individualized BGH prognosis (Figure 3). Decision curve analysis underscored the model's clinical value, showing a superior net benefit (average utility = 0.110) compared to using either the laboratory (0.102) or imaging (0.050) components in isolation (Figure 4). The DeLong test showed that the AUC of the full model was higher than that of the imaging

Table 1 Comparison of Baseline Characteristics with Different Prognoses in BGH

Variable	Favorable Outcome (n=180)	Unfavorable Outcome (n=62)	(t/X^2/Z)	P value
Demographic characteristics				
Age, years	63.00(54.00,71.00)	64.50(54.00,73.00)	−0.996	0.319
Male, n (%)	114(63.3%)	43(69.4%)	0.734	0.392
Vascular risk factors, n (%)				
Smoking history	23(12.8%)	12(19.4%)	1.613	0.204
Alcohol consumption	27(15.0%)	13(21.0%)	1.190	0.275
Hypertension	127(70.6%)	45(72.6%)	0.092	0.762
Diabetes mellitus	27(15.0%)	10(16.1%)	0.045	0.831
Coronary artery disease	32(17.8%)	13(21.0%)	0.310	0.578
Neuroimaging features, n (%)				
WMH	83(46.1%)	50(80.6%)	22.218	<0.001
LIs	80(44.4%)	46(74.2%)	16.353	<0.001
EPVS	92(51.1%)	47(75.8%)	11.504	0.001
CMB	128(71.1%)	54(87.1%)	6.320	0.012
Total load (score 3–4)	69(38.3%)	51(82.3%)	35.592	<0.001
Clinical characteristics, n (%)				
NIHSS score < 5	56(31.1%)	17(27.4%)	0.298	0.585
Hematoma volume≤10 mL	136(75.6%)	48(77.4%)	0.088	0.767
Novel biomarkers				
TG/HDL-C	1.12(0.83,1.46)	1.67(1.23,1.89)	−5.709	<0.001
Non-HDL-C	2.24(1.77,2.88)	2.99(2.27,3.52)	−4.174	<0.001
RC	−0.03(−0.88,0.51)	0.14(−0.45,0.54)	−0.940	0.347
TG/LDL-C	0.55(0.39,0.83)	0.58(0.47,0.83)	−0.776	0.438
NHHR	1.78(1.41,2.33)	2.58(2.24,3.27)	−6.558	<0.001
NLR	3.40(2.32,4.69)	3.80(2.82,5.51)	−1.882	0.060
SIRI	1.35(0.88,1.87)	2.12(1.57,2.78)	−6.336	<0.001
dNLR	0.85(0.65,0.93)	0.91(0.84,1.04)	−2.962	0.003

model (AUC: 0.929 vs. 0.720, Δ = +0.209, Z = 7.384, P < 0.001) and the biomarker model (AUC: 0.929 vs. 0.891, Δ = +0.038, Z = 2.337, P = 0.020). The AUC of the biomarker model was also higher than that of the imaging model (AUC: 0.891 vs. 0.720, Δ = +0.171, Z = 4.345, P < 0.001) (Table 4).

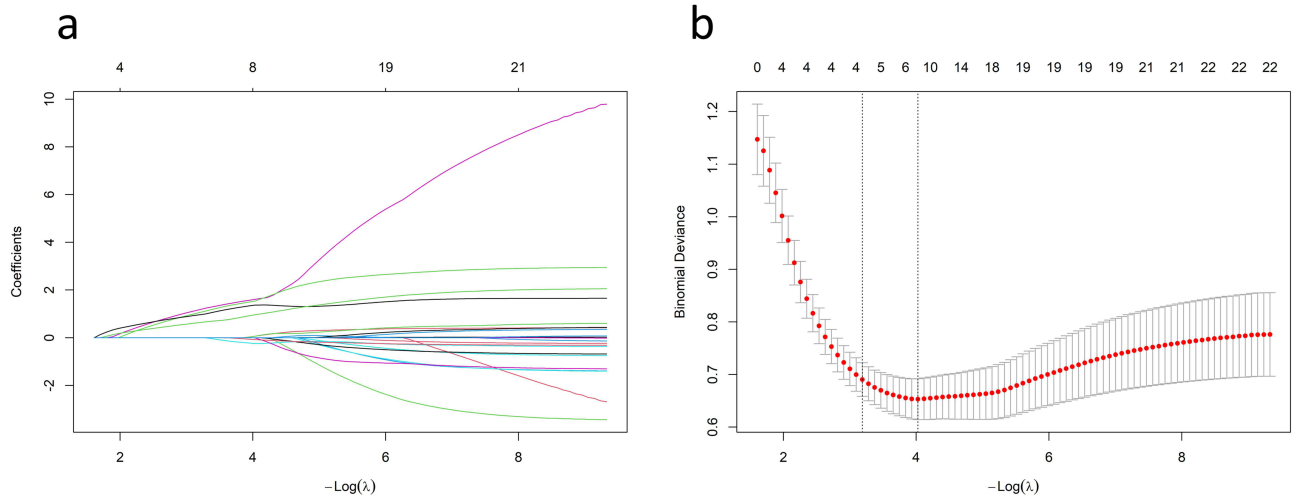

Figure 1 (**a**) Variation path of variable coefficients in the LASSO regression model with respect to -log(λ). (**b**) Tenfold cross-validation for selecting the parameter λ in the LASSO model.

https://doi.org/10.2147/IJGM.S605613

Table 2 Univariate and Multivariate Logistic Regression Analysis of Factors Affecting Prognosis in BGH Patients

Variable	Univariable Analysis		Multivariable Analysis	
	OR (95% CI)	P value	Adjusted OR (95% CI)	P value
Total load	7.46(3.64–15.29)	<0.001	9.25(3.52–24.28)	<0.001
TG/HDL-C	5.22(2.74–9.96)	<0.001	8.39(3.21–21.92)	<0.001
NHHR	5.69(3.30–9.81)	<0.001	4.95(2.50–9.82)	<0.001
SIRI	3.11(2.10–4.60)	<0.001	3.35(1.89–5.93)	<0.001

Abbreviations: OR, odds ratio; CI, confidence interval.

Table 3 ROC Curve Comparison: Analysis Comparing Predictive Models with Single Variables

Variable	AUC	95% CI	Optimal Cutoff Value	Sensitivity (%)	Specificity (%)	P Value
TG/HDL-C	0.743	0.67–0.81	1.53	66	79	<0.001
NHHR	0.779	0.70–0.86	2.19	79	70	<0.001
SIRI	0.770	0.71–0.83	2.02	63	81	<0.001
Total load	0.720	0.65–0.79	1.50	82	62	<0.001
Predictive model	0.929	0.89–0.97	0.29	86	91	<0.001

Discussion

The optimal cutoffs for TG/HDL-C ratio (≥1.53), NHHR (≥2.19), and SIRI (≥2.02) identified in our cohort are suggested to be used as risk-enhancing thresholds rather than strict diagnostic cutoffs. From a pathophysiological perspective, these thresholds are generally consistent with the ranges of reported cutoffs for insulin resistance, atherogenic lipid profiles, and systemic inflammation in the literature, suggesting a certain degree of biological plausibility. It should be noted that although these cutoffs demonstrated good predictive performance in our cohort, they may be cohort-specific; therefore, recalibration or validation may be needed when applied to other populations. Interestingly, relying solely on blood-based biomarkers already yielded a notably stronger discriminatory capacity compared to assessing radiological features alone (AUC 0.891 vs. 0.720, $P < 0.001$). However, the prognostic picture remains incomplete without structural data. When we folded the total CSVD burden into that biomarker baseline, the model's predictive accuracy experienced a tangible boost

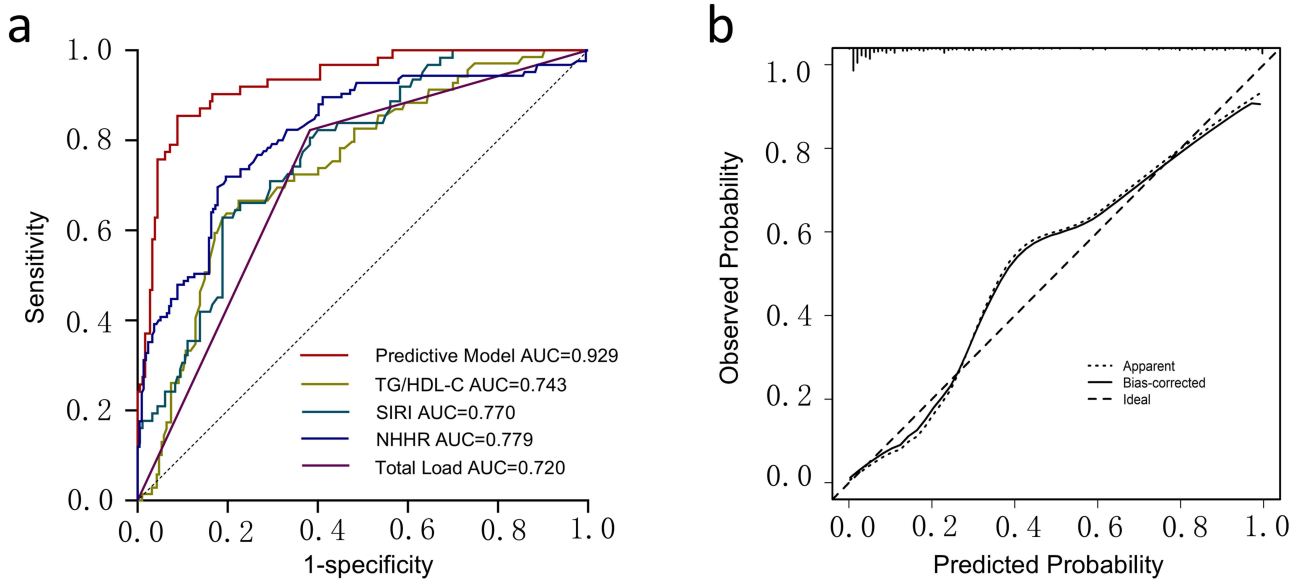

Figure 2 (**a**) ROC curves for the predictive model and individual predictors. (**b**) Calibration curves for the predictive model in the internal validation set (B=1000).

https://doi.org/10.2147/IJGM.S605613

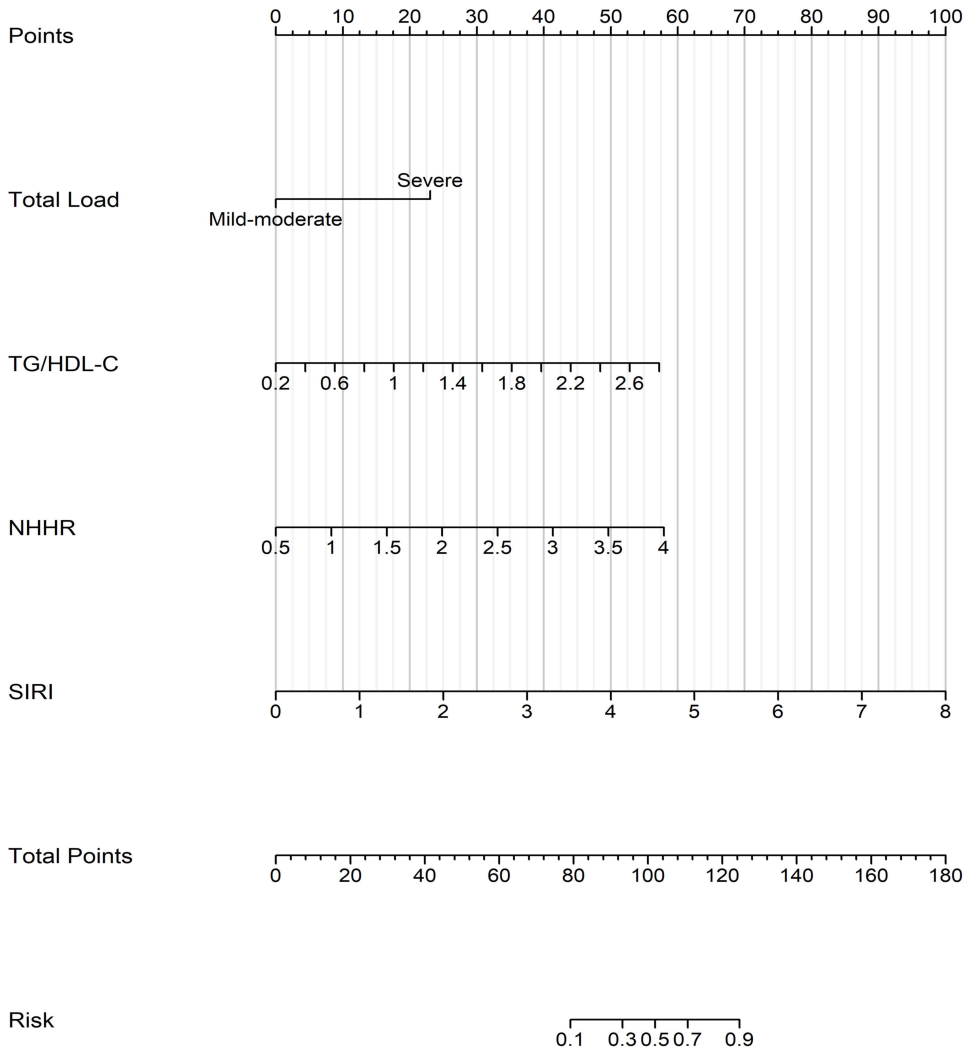

Figure 3 Nomogram for predicting the probability of poor prognosis in patients with basal ganglia hemorrhage.
Notes: To estimate the individual risk, (1) locate the patient's value on each predictor axis (total CSVD burden, TG/HDL-C ratio, NHHR, SIRI); (2) draw a vertical line upward to the "Points" scale to obtain the corresponding points for each predictor; (3) sum the points from all four predictors to obtain the total points; (4) draw a vertical line downward from the "Total Points" axis to the "Probability of poor prognosis" axis to read the predicted risk.

(ΔAUC = 0.038, P = 0.020), accompanied by a modest yet meaningful increase in net clinical benefit. What this essentially demonstrates is that structural vascular damage contributes independent warning signs that systemic metabolic and inflammatory markers simply cannot capture. Ultimately, a patient's recovery trajectory after a BGH event seems fundamentally tied to a synergistic interplay: acute systemic inflammation colliding with disrupted lipid metabolism and preexisting small vessel degradation.

Biological and Clinical Significance of Lipid and Inflammatory Biomarkers in BGH Prognosis

A classic hallmark of metabolic dysfunction is the pairing of high triglycerides with depleted HDL cholesterol. By fusing these two values, the TG/HDL-C ratio emerges as a highly sensitive barometer for lipid dysregulation—often capturing metabolic shifts much earlier than either metric could in isolation.[11] Historically, researchers have tied this specific index to a cascade of systemic issues, ranging from impaired insulin sensitivity[12] to the promotion of atherogenic profiles and broader cardiovascular vulnerability.[13] For instance, cross-sectional observations reveal that vascular rigidity scales directly with this ratio; the odds of arterial hardening escalate noticeably (OR = 1.12, 95% CI: 1.01–1.23) for every

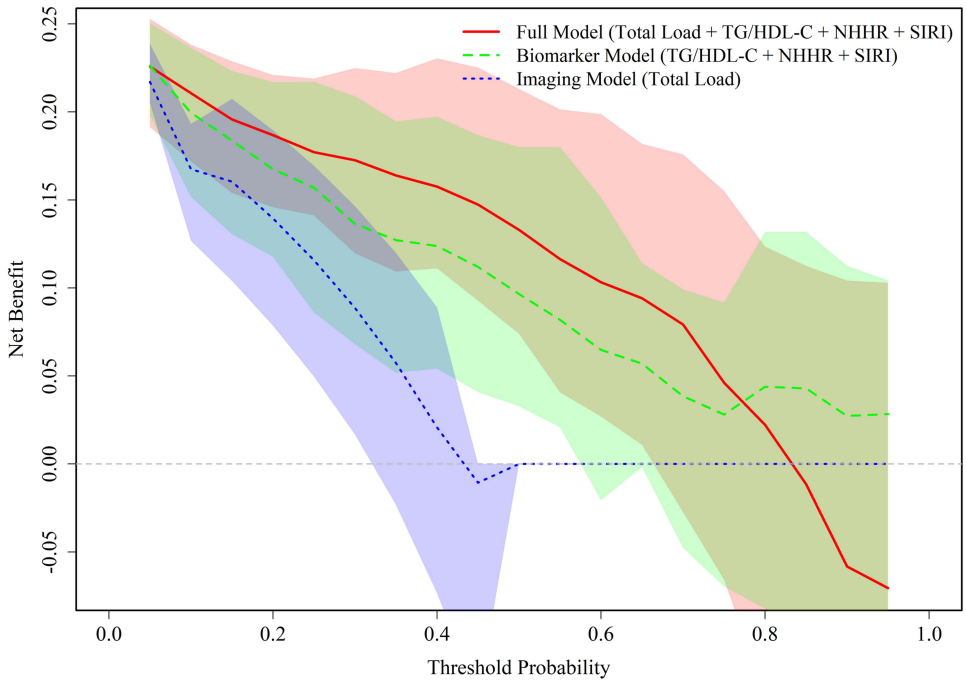

Figure 4 Decision Curve Analysis Comparing Different Models.

single unit increase.[14] When shifting the focus specifically to cerebrovascular health, the dynamic becomes slightly more complex. Data from the CHARLS cohort uncovered a distinct, non-linear trajectory in adults over 45, where stroke susceptibility climbed sharply alongside the TG/HDL-C ratio before plateauing near a 1.85 threshold.[15] Interestingly, in the highly specific context of large-vessel occlusions treated with endovascular therapy, the ratio surprisingly lost its standalone predictive power for long-term functional recovery, hinting that its true neurological influence likely depends on how it interacts with other systemic baseline factors.[16] Despite this nuance in acute interventional settings, long-term epidemiological evidence remains compelling. A ten-year longitudinal tracking effort confirmed that escalating TG/HDL-C values consistently drive up the risk for both ischemic and hemorrhagic strokes—a danger that heavily persists even in individuals who maintain a strictly normal body weight.[17] Aligning with the broader consensus of these long-term findings, our current analysis confirms that the TG/HDL-C quotient holds distinct, independent prognostic weight for BGH patients. Biologically, a severely dysregulated lipid ratio likely fuels a hostile recovery environment by exacerbating local vascular injury, driving systemic insulin resistance, and actively hindering the brain's ability to clear the hematoma, all of which ultimately pave the way for devastating functional deficits.

The NHHR metric signifies cumulative levels regarding plaque-promoting lipid particles, encompassing both very-low-density alongside low-density variants, plus residual cholesterol fractions. Contemporary observational findings derived utilizing United States mature demographics established how augmented NHHR measurements proportionally link toward increased probability concerning stroke occurrences. Furthermore, researchers uncovered a notably non-linear dose-response pattern (P = 0.002), firmly establishing that escalating concentrations of this marker heighten overall stroke susceptibility.[18] Further research has shown that elevated baseline NHHR, sustained high cumulative exposure,

Table 4 Decision Curve Analysis Comparing Different Models

Comparison	ΔAUC	Z value	P value
Full model vs Imaging model	0.209	7.384	<0.001
Full model vs Biomarker model	0.038	2.337	0.020
Biomarker model vs Imaging model	0.171	4.345	<0.001

Note: The P value was calculated using the DeLong test.

https://doi.org/10.2147/IJGM.S605613

and certain dynamic patterns of change are all associated with a higher incidence of cardiovascular disease in individuals aged 45 years and older, with a generally linear relationship observed.[19] Analysis of the NHANES database revealed distinct mortality patterns among prediabetic and diabetic populations based on their NHHR values. Specifically, researchers observed a U-shaped curve regarding overall death rates (inflection point: 2.72), alongside an L-shaped trajectory for cardiovascular-related fatalities, where the threshold was identified at 2.83.[20] Likewise, among individuals suffering minor acute cerebral infarctions, elevated NHHR concentrations appeared alongside premature mental decline 3.24 ± 1.63 vs. 3.02 ± 1.43, $P = 0.046$), every single incremental rise equated toward an escalated danger reaching 13.2% (OR = 1.13).[21,22] Our findings are consistent with these reports. In patients with BGH, elevated NHHR may indicate widespread atherosclerosis and small-vessel dysfunction, which could worsen secondary brain injury by compromising microcirculation and neural recovery. These results suggest that NHHR may have clinical value in prognostic assessment of BGH.

Accumulating evidence continuously links the SIRI to long-term functional recovery following a cerebrovascular event. Specifically, among individuals receiving intravenous thrombolysis for acute cerebral ischemia, one longitudinal analysis revealed that baseline SIRI values exceeding 1.0×10^9/L strongly forecasted unfavorable neurological status at 90 days.[23] The clinical relevance of SIRI extends directly into acute neurological settings. When researchers previously mapped this index against stroke severity, a distinct threshold (1.790×10^9/L) emerged that reliably separated mild cases from moderate-to-severe clinical presentations, ultimately flagging patients at high risk for hindered early rehabilitation.[24] This acute prognostic value is heavily reinforced by long-term epidemiological tracking. Over a ten-year observation window, seemingly healthy populations exhibiting elevated baseline SIRI values faced a tangibly steeper risk for both future cerebrovascular incidents and all-cause mortality.[25] What these overlapping timelines tell us is that this specific index acts as a highly sensitive biological mirror. Rather than just counting cells, it captures the precarious tipping point between tissue-destroying neuroinflammation and the body's necessary immune regulation during a vascular crisis. Consequently, seeing SIRI surface as a standalone predictor within our own BGH cohort makes profound biological sense. It strongly implies that the sheer intensity of a patient's systemic inflammatory cascade actively dictates their long-term recovery ceiling after the initial hemorrhage.

Recent experimental research has identified a novel upstream mechanism linking iron metabolism to neuronal injury. Stromal interaction molecule 1 (STIM1) has been shown to interact with transferrin receptor 1 (TFR1), enhancing neuronal iron uptake independently of classical calcium signaling and thereby promoting ferroptosis, a form of iron-dependent cell death that contributes to secondary injury after sICH.[26] This mechanism may help explain the prognostic relevance of TG/HDL-C, NHHR, and SIRI observed in our study. The TG/HDL-C ratio may reflect the availability of lipid substrates required for lipid peroxidation, a key step in ferroptosis. NHHR may indicate broader disturbances in lipid metabolism that accompany impaired iron regulation. SIRI may capture the inflammatory environment triggered by iron-dependent cell injury. These markers may therefore interact within a shared pathway of lipid peroxidation and inflammatory amplification, contributing to worse outcomes in BGH.

The Complementary Value of Imaging and Biomarkers

Existing literature indicates that the mere existence, as well as the advanced progression of CSVD, strongly predicts diminished physical recovery and mental decline following a cerebrovascular event. More specifically, among individuals suffering from acute cerebral ischemia, an elevated cumulative pathology score substantially correlates with detrimental clinical states one year post-onset.[27] Arba[28] reported that, after adjustment for confounding factors, total load was independently associated with poor functional outcomes at three months in patients undergoing endovascular thrombectomy (OR = 1.63, 95% CI: 1.01–2.62). Additional research highlights that an elevated cumulative lesion load strongly predicts suboptimal physical recovery following an intracerebral bleed (OR = 1.460; 95% CI, 1.02–2.10). Furthermore, extensive radiological metrics correlate with a doubled probability of subsequent cerebrovascular events (OR = 2.26; 95% CI, 1.08 to 4.72) alongside substantially shortened patient lifespans (OR = 3.140; 95% CI, 1.07–9.25; P = 0.038).[29] The profound clinical consequences of a high CSVD score were further highlighted in a recent statistical review of non-traumatic parenchymal bleeds. According to the aggregated data, advanced microvascular damage substantially drives up

the incidence of suboptimal functional recovery (57%), fatal outcomes (150%), and repeated neurological attacks (44%).[30]

Our findings are consistent with this body of evidence. The overall CSVD burden reflects the cumulative extent of small-vessel injury and structural brain damage. When a patient presents with a severe radiological footprint, it usually points to fundamentally degraded microvascular networks. This pre-existing damage severely restricts collateral blood flow and cripples the brain's natural capacity to heal post-hemorrhage—structural vulnerabilities that a simple laboratory blood draw simply cannot detect on its own. Because circulating acute-phase metrics miss this chronic physical decline, neuroimaging provides an indispensable layer of anatomical context. By treating these structural markers not as isolated findings, but as critical puzzle pieces that complement systemic blood profiles, clinicians can finally construct a truly multidimensional and accurate risk assessment for BGH recovery.

Strengths and Limitations

A potential advantage of our current research is that it attempts to move beyond traditional single-variable clinical evaluations. By exploring the combination of acute systemic inflammation, lipid measurements, and baseline CSVD radiological features, we sought to develop a potentially useful, multifaceted prognostic model for predicting recovery after BGH. Instead of depending entirely on solitary data points, this combined approach might help illustrate the ways in which circulating biological markers alongside cumulative structural tissue damage interact as related warning signs. Consequently, integrating these diverse pathophysiological elements could seemingly provide clinicians with a relatively broader, albeit preliminary, understanding regarding individual patient susceptibility.

However, the interpretation of these findings must naturally be tempered by the study's design constraints. Because our data stem from a retrospective, single-center cohort with a relatively modest sample size, there is an inherent risk of selection bias that could restrict the broader statistical power of our conclusions. Although internal validation supports the predictive reliability of the model, future external validation in larger, geographically diverse multicenter populations is needed to ensure external validity. Furthermore, our cohort was exclusively Han Chinese and predominantly featured hypertensive arteriopathy; the model's performance in other ethnic groups, in cerebral amyloid angiopathy-dominant populations, or across different severity strata remains to be validated. Biomarkers were measured only once at admission without serial monitoring, which may overlook prognostic information contained in their temporal changes. The slight S-shaped deviation in the calibration curve suggests that predicted risks should be interpreted with caution.

Conclusion

In summary, this study shows that lipid and inflammatory biomarkers, together with neuroimaging features of CSVD, are closely associated with poor outcomes in patients with BGH. The TG/HDL-C ratio, NHHR, SIRI, and total load were identified as independent predictors of unfavorable prognosis. Further research on multidimensional biomarkers may improve risk assessment and support the development of practical tools for individualized prognostic evaluation and management in patients with BGH.

Ethics Approval and Informed Consent

This study was approved by the Ethics Committee of the First Hospital of Anhui University of Science and Technology and was conducted in accordance with the Declaration of Helsinki. Written informed consent was obtained from all participants after a full explanation of the study objectives and procedures (2023-KY-B003-001).

Acknowledgments

The authors thank all clinical staff for their support.

Author Contributions

All authors made a significant contribution to the work reported, whether that is in the conception, study design, execution, acquisition of data, analysis and interpretation, or in all these areas; took part in drafting, revising or critically

reviewing the article; gave final approval of the version to be published; have agreed on the journal to which the article has been submitted; and agree to be accountable for all aspects of the work.

Funding

This study was funded and supported by the Medical Special Project of Anhui University of Science and Technology (YZ2023H1C001), the Anhui Provincial Health and Wellness Research Project Plan (AHWJ2023A20160), and the Open Fund of the Occupational Medicine and Health Joint Research Center, Institute of Health Sciences, Hefei National Comprehensive Science Center (OMH-2024-031).

Disclosure

The authors declare no conflicts of interest in this work.

References

1. Krishnamurthi RV, Ikeda T, Feigin VL. Global, regional and country-specific burden of ischemic stroke, intracerebral hemorrhage and subarachnoid hemorrhage: a systematic analysis of the global burden of disease study 2017. *Neuroepidemiology*. 2020;54(2):171–179. doi:10.1159/000506396
2. van Asch CJJ, Luitse MJA, Rinkel GJE, et al. Incidence, case fatality, and functional outcome of intracerebral haemorrhage over time, according to age, sex, and ethnic origin: a systematic review and meta-analysis. *Lancet Neurol*. 2010;9(2):167–176. doi:10.1016/S1474-4422(09)70340-0
3. Jolink WMT, Wiegertjes K, Rinkel GJE, et al. Location-specific risk factors for intracerebral hemorrhage: systematic review and meta-analysis. *Neurology*. 2020;95(13):e1807–e1818. doi:10.1212/WNL.0000000000010418
4. Samarasekera N, Fonville A, Lerpiniere C, et al. Influence of intracerebral hemorrhage location on incidence, characteristics, and outcome: population-based study. *Stroke*. 2015;46(2):361–368. doi:10.1161/STROKEAHA.114.007953
5. Lam BYK, Cai Y, Akinyemi R, et al. The global burden of cerebral small vessel disease in low- and middle-income countries: a systematic review and meta-analysis. *Int J Stroke*. 2023;18(1):15–27. doi:10.1177/17474930221137019
6. Duering M, Biessels GJ, Brodtmann A, et al. Neuroimaging standards for research into small vessel disease-advances since 2013. *Lancet Neurol*. 2023;22(7):602–618. doi:10.1016/S1474-4422(23)00131-X
7. Suzuyama K, Yakushiji Y, Ogata A, et al. Total small vessel disease score and cerebro-cardiovascular events in healthy adults: the Kashima scan study. *Int J Stroke*. 2020;15(9):973–979. doi:10.1177/1747493020908144
8. You S, Zheng D, Yoshimura S, et al. Optimum baseline clinical severity scale cut points for prognosticating intracerebral hemorrhage: INTERACT studies. *Stroke*. 2024;55(1):139–145. doi:10.1161/STROKEAHA.123.044538
9. Staals J, Makin SD, Doubal FN, et al. Stroke subtype, vascular risk factors, and total MRI brain small-vessel disease burden. *Neurology*. 2014;83(14):1228–1234. doi:10.1212/WNL.0000000000000837
10. Lau KK, Li L, Schulz U, et al. Total small vessel disease score and risk of recurrent stroke: validation in 2 large cohorts. *Neurology*. 2017;88(24):2260–2267. doi:10.1212/WNL.0000000000004042
11. Kano N, Anwardeen N, Naja K, et al. Predictive utility and metabolomic signatures of TG/HDL-C ratio for metabolic syndrome without cardiovascular disease and/or diabetes in qatari adults. *Metabolites*. 2025;15(9):574. doi:10.3390/metabo15090574
12. Murguía-Romero M, Jiménez-Flores JR, Sigrist-Flores SC, et al. Plasma triglyceride/HDL-cholesterol ratio, insulin resistance, and cardiometabolic risk in young adults. *J Lipid Res*. 2013;54(10):2795–2799. doi:10.1194/jlr.M040584
13. De Luca L, Temporelli PL, Colivicchi F, et al. Clinical impact and prognostic role of triglyceride to high-density lipoprotein cholesterol ratio in patients with chronic coronary syndromes at very high risk: insights from the START study. *Front Cardiovasc Med*. 2022;9:874087. doi:10.3389/fcvm.2022.874087
14. Zhang W, Huo W, Hu H, et al. Dose-response associations of triglyceride to high-density lipoprotein cholesterol ratio and triglyceride-glucose index with arterial stiffness risk. *Lipids Health Dis*. 2024;23(1):115. doi:10.1186/s12944-024-02095-z
15. Zhang S, Cao C, Han Y, et al. A nonlinear relationship between the triglycerides to high-density lipoprotein cholesterol ratio and stroke risk: an analysis based on data from the China Health and Retirement Longitudinal Study. *Diabetol Metab Syndr*. 2024;16(1):96. doi:10.1186/s13098-024-01339-3
16. Li J, Jiang S, Guo P, et al. TyG-BMI and TyG/BMI%: valuable evaluation tools for predicting unfavorable prognosis in ischemic stroke patients with large vessel occlusion after endovascular therapy. *J Stroke Cerebrovasc Dis*. 2025;34(8):108352. doi:10.1016/j.jstrokecerebrovasdis.2025.108352
17. Sato F, Nakamura Y, Kayaba K, et al. TG/HDL-C ratio as a predictor of stroke in the population with healthy BMI: the Jichi Medical School Cohort Study. *Nutr Metab Cardiovasc Dis*. 2022;32(8):1872–1879. doi:10.1016/j.numecd.2022.05.002
18. Ma HX, Chen HQ, Wang PC. Association between non-high-density lipoprotein cholesterol to high-density lipoprotein cholesterol ratio (NHHR) and stroke among adults in the USA: a cross-sectional NHANES study. *Biomed Environ Sci*. 2025;38(1):37–46. doi:10.3967/bes2025.001
19. Wang B, Li L, Tang Y, et al. Changes in non-high-density lipoprotein to high-density lipoprotein ratio (NHHR) and cardiovascular disease: insights from CHARLS. *Lipids Health Dis*. 2025;24(1):112. doi:10.1186/s12944-025-02536-3
20. Yu B, Li M, Yu Z, et al. The non-high-density lipoprotein cholesterol to high-density lipoprotein cholesterol ratio (NHHR) as a predictor of all-cause and cardiovascular mortality in US adults with diabetes or prediabetes: NHANES 1999-2018. *BMC Med*. 2024;22(1):317. doi:10.1186/s12916-024-03536-3
21. Wang C, Teng Z, Fan M, et al. Association between the non-high-density lipoprotein cholesterol to high-density lipoprotein cholesterol ratio and cognitive impairment in patients with cerebral small vessel disease. *Front Neurol*. 2025;16:1703244. doi:10.3389/fneur.2025.1703244
22. Wang H, Wang J, Feng D, et al. Association between the non-high-density lipoprotein cholesterol to high-density lipoprotein cholesterol ratio (NHHR) and cognitive impairment in patients with acute mild ischemic stroke. *Eur J Med Res*. 2025;30(1):430. doi:10.1186/s40001-025-02693-2

23. Ma X, Yang J, Wang X, et al. The clinical value of systemic inflammatory response index and inflammatory prognosis index in predicting 3-month outcome in acute ischemic stroke patients with intravenous thrombolysis. *Int J Gene Med*. 2022;15:7907–7918. doi:10.2147/IJGM.S384706
24. Huang L. Increased systemic immune-inflammation index predicts disease severity and functional outcome in acute ischemic stroke patients. *neurologist*. 2023;28(1):32–38. doi:10.1097/NRL.0000000000000464
25. Jin Z, Wu Q, Chen S, et al. The associations of two novel inflammation indexes, SII and SIRI with the risks for cardiovascular diseases and all-cause mortality: a ten-year follow-up study in 85,154 individuals. *J Inflamm Res*. 2021;14:131–140. doi:10.2147/JIR.S283835
26. Zhang H, Ma L, Yue Z, et al. The Ca2+ sensor STIM1 promotes neuronal ferroptosis by regulating iron homeostasis to exacerbate brain injury after intracerebral hemorrhage. *Cell Rep Med*. 2026;7:102595. doi:10.1016/j.xcrm.2026.102595
27. Georgakis MK, Fang R, Düring M, et al. Cerebral small vessel disease burden and cognitive and functional outcomes after stroke: a multicenter prospective cohort study. *Alzheimer's Dementia*. 2023;19(4):1152–1163. doi:10.1002/alz.12744
28. Arba F, D TG, Limbucci N, et al. Small vessel disease and clinical outcomes after endovascular treatment in acute ischemic stroke. *Neurol Sci*. 2019;40(6):1227–1235. doi:10.1007/s10072-019-03824-4
29. Xu M, Li B, Zhong D, et al. Cerebral small vessel disease load predicts functional outcome and stroke recurrence after intracerebral hemorrhage: a median follow-up of 5 years. *Front Aging Neurosci*. 2021;13:628271. doi:10.3389/fnagi.2021.628271
30. Cheng Z, Zhang W, Zhan Z, et al. Cerebral small vessel disease and prognosis in intracerebral haemorrhage: a systematic review and meta-analysis of cohort studies. *Eur J Neurol*. 2022;29(8):2511–2525. doi:10.1111/ene.15363